IEEE Access
Multidisciplinary | Rapid Review | Open Access Journal

Received February 18, 2020, accepted February 26, 2020, date of publication March 2, 2020, date of current version March 12, 2020.

Digital Object Identifier 10.1109/ACCESS.2020.2977434

A New Widely and Stably Adaptive Sliding-Mode Control With Nonsingular Terminal Sliding Variable for Robot Manipulators

JAEMIN BAEK[1], (Member, IEEE), WOOKYONG KWON[2], AND CHANGMOOK KANG[3], (Member, IEEE)

[1]The 1st Research and Development Institute –5rd Directorate, Agency for Defense Development (ADD), Daejeon 34186, South Korea
[2]Smart Mobility Research Section, Electronics and Telecommunications Research Institute (ETRI), Daegu 42994, South Korea
[3]Department of Electrical and Engineering, Incheon National University, Incheon 22012, South Korea

Corresponding author: Changmook Kang (mook@inu.ac.kr)

This work was supported by the Research Program (Improved Development of and Electric Power Steering System to enhance the driving stability of micro electric vehicles) funded by the Ministry of Trade, Industry and Energy (MOTIE), South Korea, under Grant 20007447.

ABSTRACT This paper presents a new widely and stably adaptive sliding-mode control (WS-ASMC) with nonsingular terminal sliding variable to enhance the performance in *reaching* and *sliding phases*. The proposed WS-ASMC has developed new widely and stably adaptive switching gains (W-ASG and S-ASG). The W-ASG is based on an adaptive law with a fast adaptation rate to appropriately suppress the errors generated by using state information from previous time. Therefore, it provides a fast convergence rate in the *reaching phase*. The S-ASG is directly designed to be related to the negative magnitude of sliding variables. It helps to enhance the system stability while providing a fast convergence rate from the W-ASG. A nonsingular terminal sliding variable is applied to the proposed WS-ASMC. It has strong attractivity and hence improves the convergence rate in the *sliding phase*. Additionally, as it exhibits a synergistic effect with the S-ASG, it is a solution to mitigate the problem of the insufficient control torque generated by applying this sliding variable. Based on these benefits, the proposed WS-ASMC can provide precise tracking performance with robustness owing to the synergistic effects of the enhanced *reaching* and *sliding phases*. It is shown that the tracking errors are uniformly ultimately bounded. The effectiveness of the proposed control is clearly demonstrated through the simulation of robot manipulators and is compared with that of existing control approaches.

INDEX TERMS Adaptive sliding-mode control, time-delayed control, nonsingular terminal sliding variable, fast adaptation, tracking control, robot manipulator.

I. INTRODUCTION

Over the last few decades, numerous studies on control approaches have been conducted, which aimed at achieving high-precision control performance of robot manipulators that are being used in a variety of industrial fields. Despite these successful works, the need for new control approaches for effectively operating robot manipulators has been emerged since various engineering fields, including nano- and bio-engineering, require much highly detailed and sophisticated controls. In other words, the precise performance may not be easily obtained by the existing control approaches. Subsequently, many researchers have recently developed various control approaches to enable the highly precise controls required by robot manipulators [1]–[5].

Among these numerous control approaches, time-delayed control (TDC) approach has received considerable attention owing to its advantage such that it does not require the information of the system model as it estimates the uncertainty of the system model using state information from previous time [6], [7]. Therefore, the TDC approach is known to be very simple and effective when applied in complex and nonlinear systems. However, an error can be generated in the process of estimating the current state information because it uses the state information from previous time, which can cause degradation in both precision and robustness of the systems.

The associate editor coordinating the review of this manuscript and approving it for publication was Zhuang Xu.

To solve this problem, auxiliary control approaches have been studied by many researchers; these include integral sliding-mode controls [8], [9], second-order sliding-mode controls [10], [11], super-twist sliding-mode controls [12], [13], boundary-layer sliding-mode controls [14], [15], and adaptive sliding-mode controls [16], [17]. TDCs with auxiliary control approaches can not only simplify the structure but also reduce the errors generated in the process of estimating the current state information. It implies that these control approaches have improved the results of the *reaching phase* described in [18]. However, there is a limit to improving the convergence rate of the *sliding phase* described in [18] because these controls use the linear sliding variable, which does not arrive at the equilibrium point in a finite time.

Studies on the sliding variables have been conducted for several decades. As one of them, the nonsingular terminal sliding variable [19]–[21], also known as the nonlinear sliding variable, has been developed to improve the convergence rate in the *sliding phase.* It could overcome the disadvantage of the linear sliding variable by ensuring that the state of the robot manipulator reaches the equilibrium point within the finite time, resulting in a fast convergence rate in the *sliding phase*. From the benefits of this sliding variable, TDCs with the nonsingular terminal sliding variable [15], [20]–[24] have been recently developed to obtain the improved convergence rate in the *sliding phase*, which continue to build on the advantages of the TDC. However, they still have the following three problems:

P1) The switching gains used in auxiliary control approaches are time-invariant [15], [20]–[23]. It implies that the robustness and tracking performance may be degraded by abruptly large errors when the reference trajectories are changed suddenly. For example, if the switching gains are inappropriately small, the tracking performance may degrade because proper switching gains cannot be generated. On the contrary, if they become inappropriately high for achieving a fast response, they may create unstable systems because of undesired side effects such as chattering. Otherwise, the switching gains used in [24] are time-varying. However, given that the switching gains are designed to generate a damping effect, it may not be able to achieve the robust tracking performance when the large errors occur abruptly.

P2) The error generated in the process of estimating the current state is called the time-delayed estimation (TDE) error. Then, to guarantee the system stability, all TDC-based control approaches must ensure the existence of an upper boundedness of the error by satisfying the stability criteria [25] of the TDC. It means that these control approaches must use the restricted TDC gains because the stability criteria is directly related to the magnitude of the TDC gains. Furthermore, the stability criteria also requires lower- and upper-bound in moment of inertia (MOI) of systems, but practicing engineers cannot have exact information of the MOI. For these reasons, these control approaches may provide degraded tracking performance and may cause system instability when applied to real systems.

P3) The high sliding gains used in the sliding variable help to provide a fast convergence rate in the *sliding phase*. However, given that the magnitude of the control torque is inversely proportional to that of the sliding gains, using a high sliding gains means that the control torque may not be sufficient to provide precise tracking performance.

To address these problems, we aim at developing a practical control approach for effective improvement in the *reaching phase* while maintaining a fast convergence rate in the *sliding phase*. In this paper, we propose a new widely and stably adaptive sliding-mode control (WS-ASMC) with nonsingular terminal sliding variable and then apply it to robot manipulators.

A1) The proposed WS-ASMC uses the state information from previous time to cancel the complex nonlinear system model and hence provides a simple structure.

Next, the proposed control scheme is designed by two new adaptive switching gains: widely adaptive switching gain (W-ASG) and stably adaptive switching gain (S-ASG).

A2) The W-ASG is developed in a well-known time-varying switching approach [26] ensuring system stability without the stability criteria of the TDC. The switching gain is closely related to the magnitude of sliding variable. For example, if the sliding variable is far away from the equilibrium point, the W-ASG generates the large value that gradually increases to make the sliding variable quickly converge to the equilibrium point. It helps to generate fast convergence rate in the *reaching phase*. However, even if a large switching gain offers such a benefit, it can cause chattering or noise amplification problems when the sliding variable stays near the equilibrium point. To solve this problem, the adaptive law of the W-ASG is designed to be reduced when the sliding variable stays near the equilibrium point. Then, as the adaptive law is inversely proportional to the magnitude of the sliding variable, the W-ASG can be adjusted while providing a fast adaptation rate without chattering.

A3) The S-ASG is developed to improve the convergence rate while enhancing the system stability around the equilibrium point. Its adaptive law is designed to be proportional to the negative magnitude of the sliding variable so that the S-ASG can reduce the undesired side effects near the equilibrium point. Besides, the S-ASG is directly combined with absolute value of the sliding variable. Therefore, the S-ASG has the effect of creating a continuous function and hence can avoid a critical problem, *e.g.*, chattering, inherent in conventional sliding-mode control.

Based on these benefits, two adaptive switching gains are extremely helpful in improving the tracking performance

while mitigating the undesired side effects and enhancing the system stability.

A4) Building upon two adaptive switching gains, the nonsingular terminal sliding variable [19] is employed in the proposed WS-ASMC. Owing to the S-ASG, although high sliding gains in the nonsingular terminal sliding variable are used to obtain a fast adaptation rate in the *sliding phase*, the proposed WS-ASMC, which is composed of inverse sliding gains, can provide a sufficient control torque while having strong attractivity.

Summarizing the above, the proposed WS-ASMC can provide precise tracking performance with enhanced robustness owing to the synergistic effects of improved performance in the *reaching* and *sliding phases*. It is shown that the tracking errors are uniformly ultimately bounded (UUB) by Lyapunov stability. The effectiveness of the proposed control is clearly explained in simulation of a robot manipulator and is compared with that of existing control approaches.

The remainder of this paper is organized as follows. In Section II, we briefly introduce what the TDC approach is. In Section III, we propose the WS-ASMC approach. In Section IV, we carry out simulations with a two-link robot manipulator. In Section V, we discuss the practical efficiency of the proposed WS-ASMC through additional simulations. In Section VI, we conclude with a brief summary of this paper.

II. TIME-DELAYED CONTROL APPROACH

In this section, we discuss the well-known TDC approach. In general, n-axes robot manipulator can be expressed as follows [27]:

$$\mathbf{M}(\mathbf{q}_t)\ddot{\mathbf{q}}_t + \mathbf{C}(\mathbf{q}_t, \dot{\mathbf{q}}_t)\dot{\mathbf{q}}_t + \mathbf{g}(\mathbf{q}_t) + \mathbf{f}(\dot{\mathbf{q}}_t) = \boldsymbol{\tau}_t - \boldsymbol{\tau}_{d,t} \quad (1)$$

where $\mathbf{q}_t \in \Re^n$, $\dot{\mathbf{q}}_t \in \Re^n$, and $\ddot{\mathbf{q}}_t \in \Re^n$ denote the angle, angular rate, and angular acceleration of each axis, respectively. $\mathbf{M}(\mathbf{q}_t) \in \Re^{n\times n}$ denotes the MOI matrix that has a positive value. $\mathbf{C}(\mathbf{q}_t, \dot{\mathbf{q}}_t)\dot{\mathbf{q}}_t \in \Re^n$ denotes the Coriolis matrix. $\mathbf{q}_t \in \Re^n$ is the gravity matrix. $\mathbf{f}(\dot{\mathbf{q}}_t) \in \Re^n$ is the friction matrix. $\boldsymbol{\tau}_t \in \Re^n$ denotes the control torque. $\boldsymbol{\tau}_{d,t} \in \Re^n$ denotes the upper-bounded external torque, *i.e.*, $\|\boldsymbol{\tau}_{d,t}\| \le d^*$ where d^* is a positive constant.

When each side of Eq. (1) is multiplied by $\mathbf{M}^{-1}(\mathbf{q}_t)$ and summarized with $\boldsymbol{\tau}_t$, we obtain

$$\begin{aligned}\boldsymbol{\tau}_t = {} & \mathbf{C}(\mathbf{q}_t, \dot{\mathbf{q}}_t)\dot{\mathbf{q}}_t + \mathbf{g}(\mathbf{q}_t) + \mathbf{f}(\dot{\mathbf{q}}_t) + \boldsymbol{\tau}_{d,t} \\ & + \big[\mathbf{M}(\mathbf{q}_t) - \bar{\mathbf{M}}\big]\ddot{\mathbf{q}}_t + \bar{\mathbf{M}}\ddot{\mathbf{q}}_t \end{aligned} \quad (2)$$

where $\bar{\mathbf{M}} \in \Re^{n\times n}$ is a positive diagonal matrix and is called "TDC gain" in this paper. Eq. (2) can be summarized to

$$\ddot{\mathbf{q}}_t = \boldsymbol{\vartheta}_t + \bar{\mathbf{M}}^{-1}\boldsymbol{\tau}_t \quad (3)$$

where $\boldsymbol{\vartheta}_t \in \Re^n$ is as follows:

$$\begin{aligned}\boldsymbol{\vartheta}_t = {} & -\bar{\mathbf{M}}^{-1}\big[\mathbf{C}(\mathbf{q}_t, \dot{\mathbf{q}}_t)\dot{\mathbf{q}}_t + \mathbf{g}(\mathbf{q}_t) + \mathbf{f}(\dot{\mathbf{q}}_t) + \boldsymbol{\tau}_{d,t}\big] \\ & - \bar{\mathbf{M}}^{-1}\big[\mathbf{M}(\mathbf{q}_t) - \bar{\mathbf{M}}\big]\ddot{\mathbf{q}}_t. \end{aligned} \quad (4)$$

As $\boldsymbol{\vartheta}_t$ in Eq. (4) is not known to practicing engineers, the estimation of $\boldsymbol{\vartheta}_t$ [28] is used, is called time-delayed estimation (TDE), which is given below:

$$\boldsymbol{\vartheta}_t \cong \boldsymbol{\vartheta}_t = \ddot{\mathbf{q}}_{t-L} - \bar{\mathbf{M}}^{-1}\boldsymbol{\tau}_{t-L} \quad (5)$$

where L denotes a sufficiently small sampling time. From Eq. (5), the TDC approach [7] can be expressed as follows:

$$\boldsymbol{\tau}_t^C = -\bar{\mathbf{M}}\ddot{\mathbf{q}}_{t-L} + \boldsymbol{\tau}_{t-L}^C + \bar{\mathbf{M}}(\ddot{\mathbf{q}}_{d,t} + \mathbf{K}_d\dot{\mathbf{e}}_t + \mathbf{K}_p\mathbf{e}_t) \quad (6)$$

where $\mathbf{e}_t = \mathbf{q}_{d,t} - \mathbf{q}_t \in \Re^n$ denotes the angular error in the robot manipulator. $\boldsymbol{\tau}_t^C \in \Re^n$ denotes the control torque generated by the TDC approach. $\mathbf{K}_d \in \Re^{n\times n}$ and $\mathbf{K}_p \in \Re^{n\times n}$ are positive diagonal matrices for a pole arrangement.

Substituting Eq. (6) into Eq. (3) yields the error dynamics as follows:

$$\ddot{\mathbf{e}}_t + \mathbf{K}_d\dot{\mathbf{e}}_t + \mathbf{K}_p\mathbf{e}_t + \mathbf{E}_t = 0 \quad (7)$$

where $\dot{\mathbf{e}}_t = \dot{\mathbf{q}}_{d,t} - \dot{\mathbf{q}}_t \in \Re^n$ and $\ddot{\mathbf{e}}_t = \ddot{\mathbf{q}}_{d,t} - \ddot{\mathbf{q}}_t \in \Re^n$ denote the angular velocity error and angular acceleration error in the robot manipulator, respectively. $\mathbf{E}_t = \boldsymbol{\vartheta}_t - \boldsymbol{\vartheta}_{t-L} = (E_{1,t}, E_{2,t}, \cdots, E_{n,t})^T \in \Re^n$ is called a TDE error. Here, the upper bound of $\mathbf{E}_t$ must exist to ensure the system stability of the robot manipulator. To guarantee the upper bound of $\mathbf{E}_t$, *i.e.*, $\|\mathbf{E}_t\| \le \bar{E}^*$ where $\bar{E}^*$ is a positive value, the TDC approach must satisfy the following stability criteria [7], [29]:

$$\|\mathbf{I} - \mathbf{M}^{-1}(\mathbf{q}_t)\bar{\mathbf{M}}\| < 1 \quad (8)$$

where $\mathbf{I} \in \Re^{n\times n}$ denotes a unit matrix. The proof of Eq. (8) can be found in [25].

In Eq. (8), the TDC gain $\bar{\mathbf{M}}$ means that a gain of a restricted magnitude must always be used in the robot manipulator. Given that it affects the magnitude of $\boldsymbol{\tau}_t^C$ as in Eq. (6), it may not be easy to suppress the TDE error $\mathbf{E}_t$. In other words, it implies that it has a lot of room for improper TDC gain, which may provide a result of degraded tracking performance. Furthermore, the TDC gain $\bar{\mathbf{M}}$ is directly related to the magnitude of the MOI. However, it is almost impossible for practicing engineers to know the MOI, and thus this is closely connected to the aspect of "*practicality*" in real systems. Also, Eq. (7) shows mathematically that $\mathbf{q}_t$ reaches $\mathbf{q}_{d,t}$ asymptotically when the TDE error $\mathbf{E}_t$ is suppressed. It implies that $\mathbf{q}_t$ does not reach $\mathbf{q}_{d,t}$ in a finite time, and the convergence rate is lowered in the vicinity of the equilibrium point.

III. PROPOSED WS-ASMC APPROACH

In this section, we introduce the proposed WS-ASMC approach, which can be expressed as follows:

$$\begin{aligned}\boldsymbol{\tau}_t^P = {} & -\bar{\mathbf{M}}\ddot{\mathbf{q}}_{t-L} + \boldsymbol{\tau}_{t-L}^P + \bar{\mathbf{M}}\big[\ddot{\mathbf{q}}_{d,t} + \frac{q}{p}\mathbf{K}_s^{-1}\dot{\mathbf{e}}_t^{2-\frac{p}{q}}\big] \\ & + \bar{\mathbf{M}}\big[\hat{\mathbf{K}}_t^S + \hat{\mathbf{K}}_t^E\big]\mathrm{sgn}(\mathbf{s}_t) \end{aligned} \quad (9)$$

where $\boldsymbol{\tau}_t^P \in \Re^n$ denotes the control torque generated by the proposed WS-ASMC approach. $\mathbf{K}_s = \mathrm{diag}(K_{s,1}, K_{s,2}, \cdots, K_{s,n}) \in \Re^{n\times n}$ is the positive diagonal

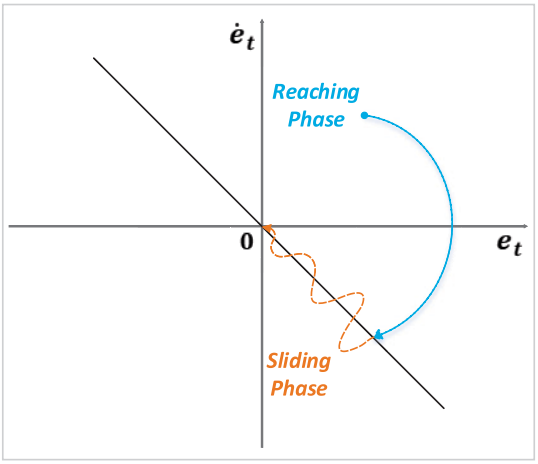

FIGURE 1. The behavior of the reaching and sliding phases in the proposed WS-ASMC.

matrix to be determined for adjusting the convergence rate in the *sliding phase*, which is called sliding gain in this paper.

To improve the convergence rate in the *reaching phase* (Figure 1), two adaptive switching gains are employed: $\hat{\mathbf{K}}_t^E$ and $\hat{\mathbf{K}}_t^S$. $\hat{\mathbf{K}}_t^E = \text{diag}(\hat{k}_{1,t}^E, \hat{k}_{2,t}^E, \cdots, \hat{k}_{n,t}^E) \in \Re^{n\times n}$ [26] whose $\hat{k}_{i,t}^E$ is defined as follows:

$$\hat{k}_{i,t}^E = \hat{k}_{0,i,t}^E + \bar{k}_{1,i}\|\dot{\mathbf{q}}_t\|^2 + \bar{k}_{2,i}\|\ddot{\mathbf{q}}_t - \ddot{\mathbf{q}}_{t-L}\| + \bar{k}_{3,i}\|\ddot{\mathbf{q}}_t\| \quad (10)$$

where $\bar{k}_{1,i}$, $\bar{k}_{2,i}$, and $\bar{k}_{3,i}$ are positive design parameters to be determined properly for suppressing the TDE error as described in Appendix A. $\hat{k}_{0,i,t}^E$ is called widely adaptive switching gain (W-ASG) in this paper whose adaptive law is as follows:

$$\dot{\hat{k}}_{0,i,t}^E = \begin{cases} \phi_i\left[\gamma_i^{-1}|s_{i,t}|\right]^{\mathcal{L}_t}\eta_{i,t}\mathcal{L}_t, & \text{if } \hat{k}_{0,i,t}^E > \underline{k}_{0,i}^{*,E} \\ \phi_i\left[\gamma_i^{-1}|s_{i,t}|\right]\eta_{i,t}, & \text{if } \hat{k}_{0,i,t}^E = \underline{k}_{0,i}^{*,E} \end{cases} \quad (11)$$

for $\mathcal{L}_t = \text{sgn}(\|\mathbf{s}_t\|_\infty - \varepsilon) \in \Re$ where ε is the positive boundedness parameter. ϕ_i and γ_i are the positive design parameters for adjusting the adaptation rate of $\hat{k}_{0,i,t}^E$. $\eta_{i,t} = \frac{p}{q}K_{s,i}\dot{e}_{i,t}^{\frac{p}{q}-1}$ for positive odd integers p and q where $1 < \frac{p}{q} < 2$. $\underline{k}_{0,i}^{*,E}$ is set to be a small positive constant for maintaining $\hat{k}_{0,i,t}^E$ with positive value.

As shown in Eq. (11), $\hat{k}_{0,i,t}^E$ can be adjusted for suppressing the TDE error, which has two different forms according to the $\mathcal{L}_t$, *e.g.*, $\|\mathbf{s}_t\|_\infty \geq \varepsilon$ and $\|\mathbf{s}_t\|_\infty < \varepsilon$. For $\|\mathbf{s}_t\|_\infty \geq \varepsilon$, $\hat{k}_{0,i,t}^E$ increases for a fast convergence rate of the *reaching phase* until all sliding variables reach a fixed boundedness ε of the vicinity of the sliding manifold. After that, $\hat{k}_{0,i,t}^E$ decreases for avoiding chattering while staying at $\|\mathbf{s}_t\|_\infty < \varepsilon$. However, its adaptation rate may decrease slowly because the adaptive law of $\hat{k}_{0,i,t}^E$ is designed to be dominant in terms of the magnitude of the sliding variable, which can cause chattering. To solve this problem, the adaptive law is designed to be inversely proportional to the magnitude of the sliding variable, which exhibits a fast adaptation rate. For this reason, although $\hat{k}_{0,i,t}^E$ has high switching gain temporarily, it provides a fast convergence rate in the *reaching phase* without chattering.

As one of two adaptive switching gains, it represents $\hat{\mathbf{K}}_t^S = \text{diag}(\hat{k}_{1,t}^S, \hat{k}_{2,t}^S, \cdots, \hat{k}_{n,t}^S) \in \Re^{n\times n}$ whose $\hat{k}_{i,t}^S$ is defined as follows:

$$\hat{k}_{i,t}^S = \hat{k}_{0,i,t}^S|s_{i,t}| \quad (12)$$

where $\hat{k}_{0,i,t}^S$ is called stably adaptive switching gain (S-ASG) in this paper. Its adaptive law is as follows:

$$\dot{\hat{k}}_{0,i,t}^S = \begin{cases} -\delta_i|s_{i,t}|^a - \delta_i\omega_i|s_{i,t}|^a, & \text{if } \hat{k}_{0,i,t}^S = \bar{k}_{0,i}^{*,S} \\ -\delta_i|s_{i,t}|^a - \delta_i\omega_i|s_{i,t}|^a\mathcal{L}_t, & \text{if } \underline{k}_{0,i}^{*,S} < \hat{k}_{0,i,t}^S < \bar{k}_{0,i}^{*,S} \\ -\delta_i|s_{i,t}|^a + \delta_i\omega_i|s_{i,t}|^a, & \text{if } \hat{k}_{0,i,t}^S = \underline{k}_{0,i}^{*,S} \end{cases} \quad (13)$$

where δ_i and a are positive design parameters for adjusting the adaptation rate of $\hat{k}_{0,i,t}^S$. Then, ω_i should be set larger than 1, *i.e.*, $\omega_i > 1$. $\underline{k}_{0,i}^{*,S}$ is set to maintain $\hat{k}_{0,i,t}^S$ with a low positive value. $\bar{k}_{0,i}^{*,S}$ is defined as the maximum value of $\hat{k}_{0,i,t}^S$.

As shown in Eq. (13), the adaptive law is composed of two terms. The first term $-\delta_i|s_{i,t}|^a$ stands for a damping term, and the second term $-\delta_i\omega_i|s_{i,t}|^a\mathcal{L}_t$ stands for a leakage term. These terms are designed to be proportional to the negative magnitude of the sliding variable and then can adjust $\hat{k}_{0,i,t}^S$ appropriately. For $\|\mathbf{s}_t\|_\infty \geq \varepsilon$, $\hat{k}_{0,i,t}^S$ decreases until it reaches its low bound because it works mainly in the W-ASG. On the other hand, for $\|\mathbf{s}_t\|_\infty < \varepsilon$, $\hat{k}_{0,i,t}^S$ increases to compensate the convergence rate near equilibrium point. $\hat{k}_{0,i,t}^S$ does not cause undesired side effects owing to the damping term. Moreover, since it consists of a product of sliding variable as shown in Eq. (12), $\hat{k}_{i,t}^S$ does not cause the chattering problem even though any positive $\hat{k}_{0,i,t}^S$ exists.

To improve convergence rate in the *sliding phase* (Figure 1), we employ sliding variable $\mathbf{s}_t = (s_{1,t}, s_{2,t}, \cdots, s_{n,t})^T \in \Re^n$ expressed in the following form:

$$\mathbf{s}_t = \mathbf{e}_t + \mathbf{K}_s(\dot{\mathbf{e}}_t)^{\frac{p}{q}} \quad (14)$$

where it is called nonsingular terminal sliding variable [19]. $\text{sgn}(\mathbf{s}_t) = [\text{sgn}(s_{1,t}), \text{sgn}(s_{2,t}), \cdots, \text{sgn}(s_{n,t})]^T \in \Re^n$ is a signum function in Eq. (9) which is defined as

$$\text{sgn}(s_{i,t}) = \begin{cases} 1 & \text{if } s_{i,t} \geq 0 \\ -1 & \text{if } s_{i,t} < 0 \end{cases} \quad (15)$$

for all $i = 1, 2, \cdots, n$.

The larger the sliding gain $\mathbf{K}_s$ is set, the faster the tracking error $\mathbf{e}_t$ described in Eq. (14) converges to the equilibrium point. However, since control approaches based on nonsingular terminal sliding variables use the inverse sliding gain directly, they may result in system instability. Although the proposed WS-ASMC is also based on nonsingular terminal sliding variables, Eqs. (12) and (13) help the proposed WS-ASMC generate sufficient output torque. To be summarized, $\hat{k}_{i,t}^S$ can guarantee the system stability while improving the convergence rate of the *sliding phase*.

To provide an overall structure of the proposed WS-ASMC, its schematic diagram is described in Figure 2.

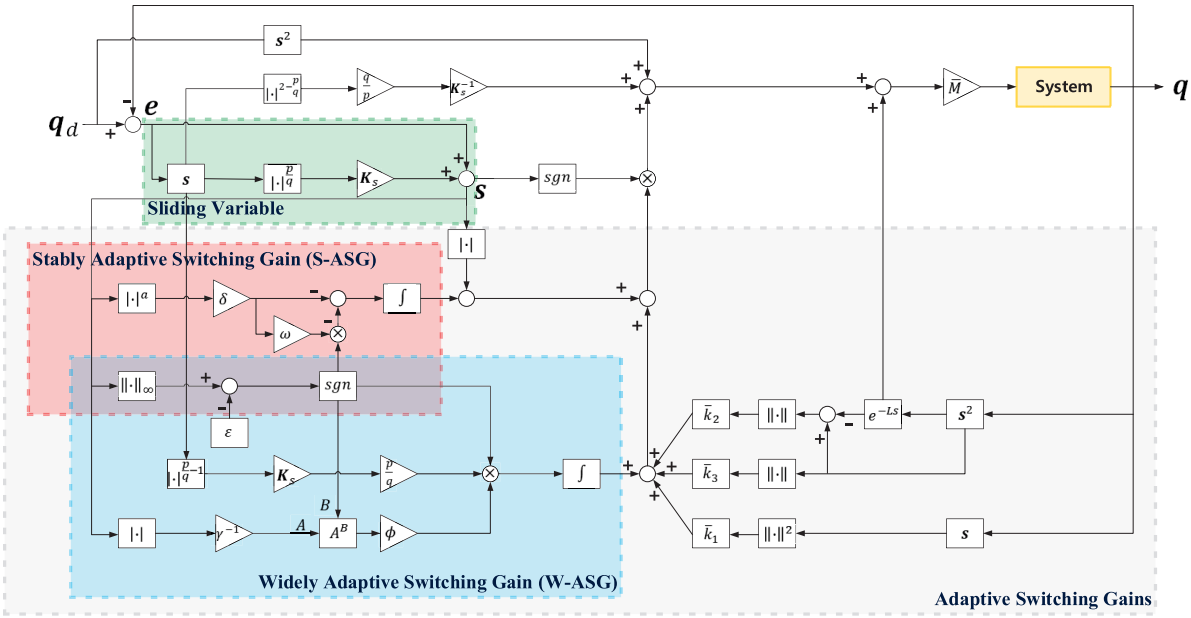

FIGURE 2. A schematic diagram of the proposed WS-ASMC.

As shown in Eqs. (11) and (13), these adaptive laws of two adaptive switching gains are strongly affected by the fixed boundedness ε. The boundedness is directly related to the magnitude of the sliding variable.

Theorem 1: For the system model in Eq. (1), the proposed WS-ASMC in Eq. (9) allows the sliding variable $\mathbf{s}_t$ *to fall within the boundedness* ε *that exists in the vicinity of the sliding manifold at the finite time* $t_s > 0$*. Then, the sliding variable* $\mathbf{s}_t$ *is guaranteed to be UUB for* $t \geq t_s$ *as follows*:

$$\|\mathbf{s}_t\| < \sqrt{\sum_{i=1}^{n} \varepsilon^2 + \chi_1 + \chi_2}$$

where

$$\chi_{1,t} = \sum_{i=1}^{n} \frac{\gamma_i}{\phi_i} \left[\max_i \left(\bar{E}_{0,i}^*, \left| \bar{k}_{0,i}^{*,E} - \bar{E}_{0,i}^* \right| \right) \right]^2$$

$$\chi_{2,t} = \sum_{i=1}^{n} \frac{1}{\delta_i} \left(\bar{k}_{0,i}^{*,S} \right)^2.$$

Proof: The proof is given in Appendix A. □

Lemma 1: For the system model in Eq. (1), the widely adaptive switching gain $\hat{k}_{0,i,t}^{E}$ *has the unknown upper-bound* $\bar{k}_{0,i}^{*,E}$ *that is a positive constant as follows*:

$$\hat{k}_{0,i,t}^{E} \leq \bar{k}_{0,i}^{*,E}$$

for $t \geq 0$.

Proof: The proof is given in Appendix B. □

Lemma 2: For the system model in Eq. (1), the TDE error $\mathbf{E}_t$ *is derived from the reasonable assumptions in [26], whose time-varying bound consists of four positive constants,* i.e., $\bar{E}_0^*$, $\bar{E}_1^*$, $\bar{E}_2^*$, *and* $\bar{E}_3^*$, *as follows*:

$$\|\mathbf{E}_t\| \leq \bar{E}_0^* + \bar{E}_1^* \|\dot{\mathbf{q}}_t\|^2 + \bar{E}_2^* \|\ddot{\mathbf{q}}_t - \ddot{\mathbf{q}}_{t-L}\| + \bar{E}_3^* \|\ddot{\mathbf{q}}_t\|$$

for $t \geq 0$.

Proof: The proof is given in [26]. □

Remark 1: As a solution to reduce the chattering, the boundary-layer approach [30]–[32] is well-known, which helps to generate the continuous function instead of the signum function (15). This control approach is simple and effective in relation to the chattering reduction. However, it may provide the slow convergence rate in the vicinity of the equilibrium point. On the other hand, the proposed WS-ASMC (9) makes the chattering-free results owing to the W-ASG with the fast adaptation rate and the S-ASG with the damping term even when using the signum function. Moreover, the proposed WS-ASMC offers the fast convergence rate in the vicinity of the equilibrium point.

IV. SIMULATION

A. SIMULATION SETUP

To illustrate the effectiveness of the proposed WS-ASMC, we conduct simulations with a two-link planar robot manipulator in Appendix C. The parameters of the proposed WS-ASMC in Eq. (9) are set as $K_{s,1} = K_{s,2} = 1.2 \times 10^{-1}$, $p = 5$, $q = 3$, $L = 10^{-3}$, $\bar{M}_1 = 10^{-2}$, $\bar{M}_2 = 2 \times 10^{-3}$, $\phi_1 = \phi_2 = 10^4$, $\gamma_1 = \gamma_2 = 10$, $\varepsilon = 10^{-1}$, $\delta_1 = 2 \times 10^3$, $\delta_2 = 2.5 \times 10^3$, $\omega_1 = \omega_2 = 11 \times 10^{-1}$, $a = 0.03$, $\bar{k}_{1,1} = \bar{k}_{1,2} = \bar{k}_{1,3} = 10^{-1}$, $\bar{k}_{2,1} = \bar{k}_{2,2} = \bar{k}_{2,3} = 25 \times 10^{-1}$, $\underline{k}_{0,1}^{*,S} = \underline{k}_{0,2}^{*,S} = 10^3$, and $\bar{k}_{0,1}^{*,S} = \bar{k}_{0,2}^{*,S} = 2 \times 10^3$.

B. SIMULATION DESCRIPTION

The purpose of the simulation is to make the angle of joints 1 and 2 in the robot manipulator $\mathbf{q}_t$ follow the reference trajectory $\mathbf{q}_{d,t}$. The reference trajectory (Figure 3) has a non-differentiable point and then changes from low-to-high movement. Moreover, as an external factor, additional payload is applied to the end-effector of the robot manipulator.

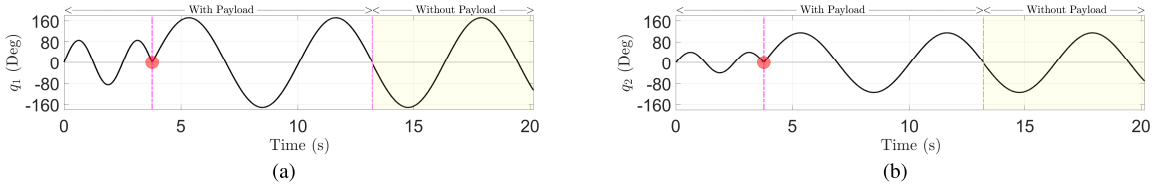

FIGURE 3. Trajectories of the desired reference: (a) Joint 1. (b) Joint 2.

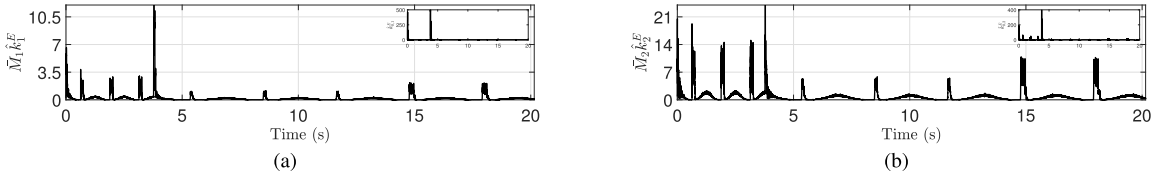

FIGURE 4. W-ASG and Eq. (10) of the proposed WS-ASMC: (a) Joint 1. (b) Joint 2.

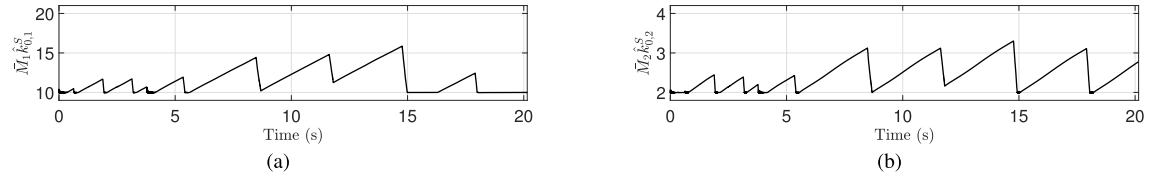

FIGURE 5. S-ASG of the proposed WS-ASMC: (a) Joint 1. (b) Joint 2.

In this simulation, we will focus on three points as follows:

- Nominal tracking performance affected by undesired side effects such as Coulomb friction [33]
- Chattering phenomena and convergence rate affected by a non-differentiable point in the reference trajectory
- Robust tracking performance affected by the reference trajectory with and without payload on the end-effector of the robot manipulator.

To illustrate the effectiveness of the proposed WS-ASMC in these points,

- Time-delayed control (TDC) [7]
- Model-free nonsingular terminal sliding-mode control (MNTSMC) [22]

are employed for comparison. All parameters of these control approaches, *e.g.,* TDC, MNTSMC, and the proposed WS-ASMC, are tuned in the reference trajectory on the robot manipulator with payload. The parameter tuning procedure is introduced in Appendix D.

C. SIMULATION RESULTS

Figure 4 shows the W-ASG and Eq. (10) of the proposed WS-ASMC. The W-ASG is an adaptive variable of a time-varying gain $\hat{k}_{i,t}^E$ in Eq. (10). Since adaptive law in Eq. (11) is directly related to the magnitude of the sliding variable, the W-ASG tends to provide high switching gain when the sliding variable moves away from the sliding manifold. On the other hand, the adaptive law is inversely related to the magnitude of the sliding variable when the sliding variable stays near the sliding manifold. Therefore, the W-ASG tends to produce low switching gain through a fast adaptation rate to avoid undesired side effects such as chattering. It is observed as follows:

- When the motion direction of motor in the robot manipulator changes, Coulomb friction forces adverse effects such as system instability and fluctuation, which causes degraded tracking performance with less robustness, *e.g.,* 1 s, 2 s, 3 s, 3.7 s, 5 s, 9 s, 12 s, 15 s, and 18 s, as shown in Figure 3.

As observed in Figure 4, the W-ASG offers high switching gain to suppress the above-mentioned problems at the non-differentiable point in 3.77 s. The W-ASG is also changed adaptively to achieve desired tracking in other points but is relatively small-adjusted. Other variables in Eq. (10), except for the W-ASG, are further implemented to suppress undesired side effects in other points. It seems to be a change in low frequency compared with the W-ASG, but it helps to achieve better tracking performance while reducing undesired side effects when the sliding variable stays in the vicinity of the sliding manifold, as shown in Figure 8.

Figure 5 shows the S-ASG of the proposed WS-ASMC that is an adaptive variable of a time-varying gain $\hat{k}_{i,t}^S$ in Eq. (12). The S-ASG, unlike the W-ASG, has a slow adaptation rate due to the damping term used in Eq. (13). Therefore, it may not be as powerful as the W-ASG with regard to the convergence rate. However, as the S-ASG provides the effect of having a continuous function owing to absolute value of the sliding variable, it can be operated for assisting the convergence rate while maintaining the system stability when the sliding variable stays around sliding manifold. It is a result that it helps to provide the improved tracking performance at points where the direction of motion of the motor in the robot manipulator does not change, as shown in Figure 8.

Figure 6 shows the control inputs of the proposed WS-ASMC that is chattering-free. However, it can be

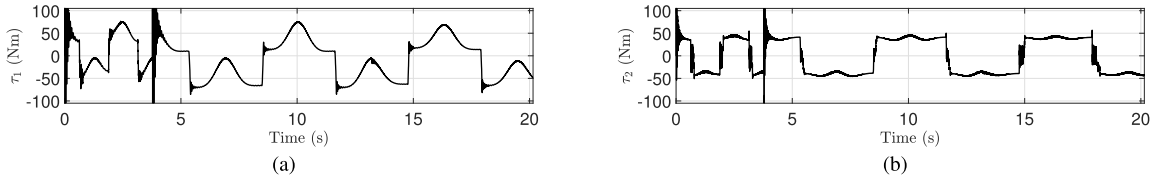

FIGURE 6. Control inputs of the proposed WS-ASMC: (a) Joint 1. (b) Joint 2.

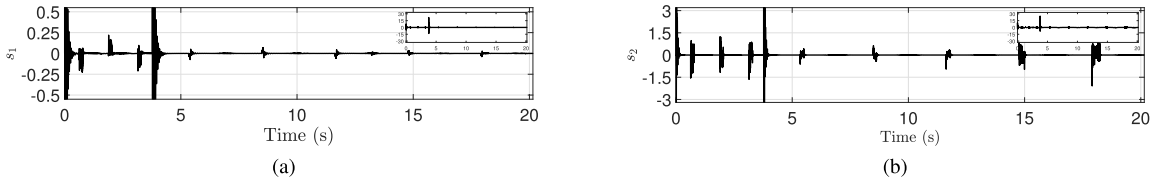

FIGURE 7. Sliding variables of the proposed WS-ASMC: (a) Joint 1. (b) Joint 2.

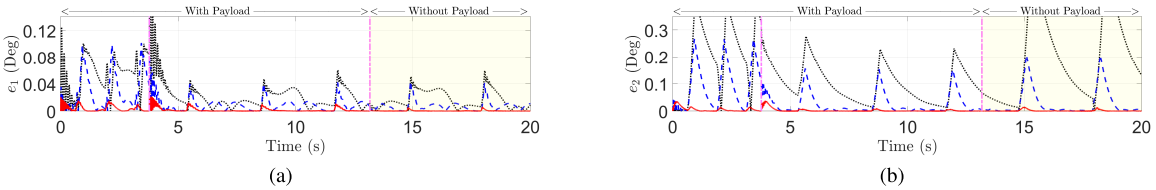

FIGURE 8. Comparison of the tracking errors of TDC (dotted-line), MNTSMC (dashed-line), and the proposed WS-ASMC (solid-line): (a) Joint 1. (b) Joint 2.

observed that the control input oscillation occurs at some points. As shown in Figure 3, the reference trajectory has a non-differential point at 3.77 s. Then, the proposed WS-ASMC produces a very large W-ASG instantaneously to suppress critical disturbances and hence the fast adaptation rate of the W-ASG seems to cause the control input oscillation. In other words, it is a behavior to achieve the desired tracking performance and hence is not an inherent problem of the proposed WS-ASMC. In the vicinity of 15 s and 18 s, it is more likely to generate the control input oscillation in Figure 6(b) than Figure 6(a). It is an effort of the W-ASG to reduce undesired side effects on the friction generated by the change of the motion direction of robot manipulator. It means that it is the behavior of the W-ASG to improve robust tracking performance. It can be confirmed that the tracking error is reduced without chattering, as shown in Figure 8.

Figure 7 shows the sliding variables of the proposed WS-ASMC. When the sliding variable leaves the vicinity of sliding manifold, it is strongly influenced by the W-ASG. On the other hand, when the sliding variable stays in the vicinity of sliding manifold, it is mainly influenced by the S-ASG. Therefore, the effect on the sliding variable tends to be similar to the tracking error, as shown in Figure 8.

Figure 8 shows the tracking errors of TDC, MNTSMC, and the proposed WS-ASMC. To begin with, it can be easily observed that the proposed WS-ASMC is superior to other control approaches because the proposed control has powerful activities to maintain a fast convergence rate while suppressing the TDE error owing to above-mentioned figures. In particular, even though critical side effects are generated by a non-differential point, the proposed WS-ASMC provides better tracking performance than other control approaches owing to the proposed W-ASG and S-ASG. The root-mean-square (RMS) values of the tracking errors are given in Table 1.

TABLE 1. The RMS values of tracking errors.

Control Strategies	Joint 1 (Deg)	Joint 2 (Deg)
TDC [7]	3.67×10^{-2}	20.31×10^{-2}
MNTSMC [22]	2.08×10^{-2}	7.04×10^{-2}
Proposed WS-ASMC (9)	0.34×10^{-2}	0.62×10^{-2}

V. DISCUSSION

A. SIMULATION DESCRIPTION

The purpose of the discussion is to further illustrate the positive effects of the proposed WS-ASMC through the additional simulations. The reference trajectory (Figure 9) has a sinusoidal function that allows a smooth motion. The rate of the reference trajectory (Figure 9) is 1.5 times faster than that of the reference trajectory (Figure 3), and the amplitude of the reference trajectory (Figure 9) is also set larger than that of the reference trajectory (Figure 3). Then, two additional external torques are generated to disturb the motion of the robot manipulator, which instantaneously produce 150 Nm in 2 s and 300 Nm in 7 s, as shown in Figure 10.

In this section, we will focus on two points as follows:

- Nominal tracking performance generated by the reference trajectory with a fast frequency
- Robust tracking performance affected by external torques.

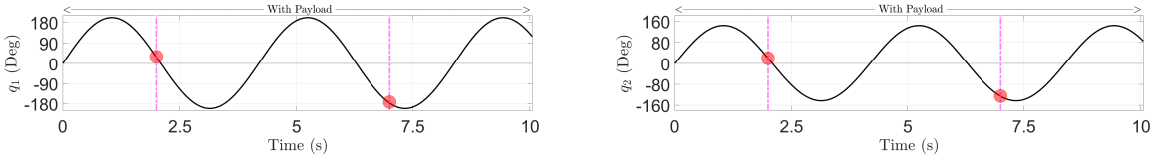

FIGURE 9. Trajectories of the desired reference: (a) Joint 1. (b) Joint 2.

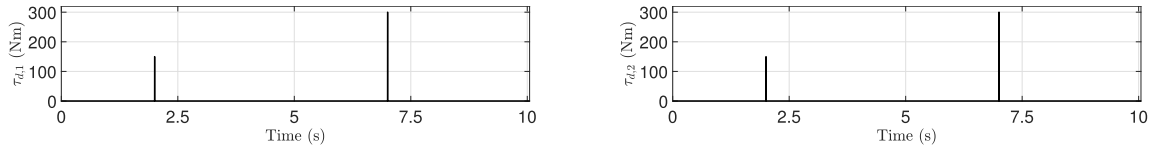

FIGURE 10. External torques generated in robot manipulator: (a) Joint 1. (b) Joint 2.

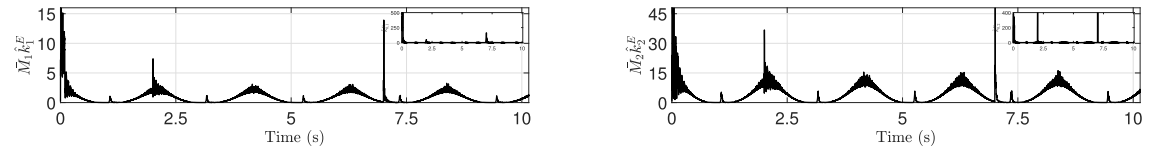

FIGURE 11. W-ASG and Eq. (10) of the proposed WS-ASMC: (a) Joint 1. (b) Joint 2.

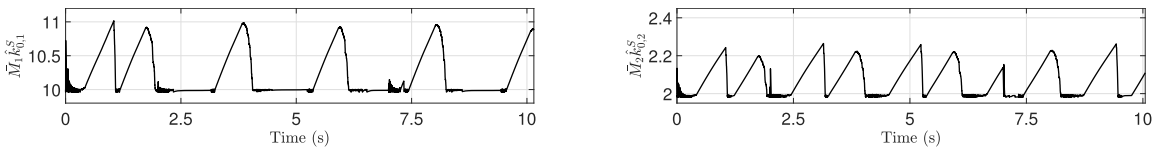

FIGURE 12. S-ASG of the proposed WS-ASMC: (a) Joint 1. (b) Joint 2.

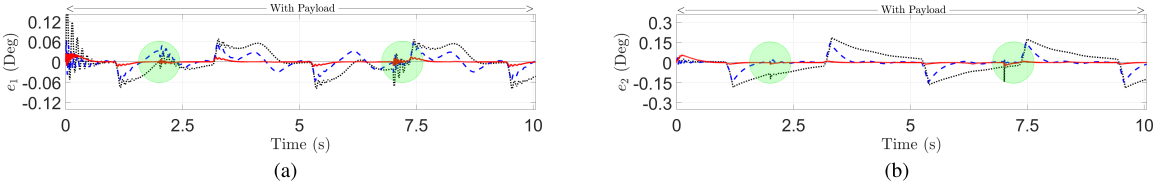

FIGURE 13. Comparison of the tracking errors of TDC (dotted-line), MNTSMC (dashed-line), and the proposed WS-ASMC (solid-line): (a) Joint 1. (b) Joint 2.

To illustrate fairly the effectiveness of the proposed WS-ASMC in these points, the control approaches [7], [22] used in Section IV are employed for comparison. The parameter values of all control approaches, including the proposed WS-ASMC, are the same as those set in Section IV.

B. SIMULATION RESULTS

Figure 11 shows the W-ASG and Eq. (10) of the proposed WS-ASMC. Given that the W-ASG can move dynamically owing to a fast adaptation rate, it offers the powerful switching gains to suppress the undesirable side effects when the unsuspected disturbances, *i.e.,* strong external torques, occur to the robot manipulator. In other words, even if the large disturbances are unexpectedly generated as in Figure 10, the W-ASG can offset them owing to its high switching gains. Other variables in Eq. (10), except for the W-ASG, are implemented to make the desired tracking responses for the reference trajectory with a fast frequency. It seems to be a change in low frequency, but it helps to obtain better tracking performance while reducing undesired side effects, as shown in Figure 13.

Figure 12 shows the S-ASG of the proposed WS-ASMC. As observed in Figure 12, the S-ASG may not be as powerful as the W-ASG with regard to the adaptation rate because it has the damping term. For this reason, it may be slow to respond appropriately to strong external torques. However, the effect of the damping term can be operated for assisting the convergence rate in the transient fields except for 2 s and 7 s in Figure 9. As a result, it helps to improve the tracking performance at points except for unsuspected disturbances, as shown in Figure 13.

Figure 13 shows the tracking errors of TDC, MNTSMC, and the proposed WS-ASMC. It can be observed that the proposed WS-ASMC is superior to other control approaches even if the reference trajectory with a fast frequency is accompanied by the strong external torques.

TABLE 2. The RMS values of tracking errors.

Control Strategies	Joint 1 (Deg)	Joint 2 (Deg)
TDC [7]	3.68×10^{-2}	8.99×10^{-2}
MNTSMC [22]	2.04×10^{-2}	4.21×10^{-2}
Proposed WS-ASMC (9)	0.51×10^{-2}	0.91×10^{-2}

Moreover, compared with Figure 8, the proposed WS-ASMC represents no significant difference in overall tracking errors, unlike other control approaches. Besides, the proposed WS-ASMC offers overwhelming tracking performance over other control approaches at points close to 2 s and 7 s. From these results, it can be observed that the proposed WS-ASMC improves more robust tracking performance than other control approachers owing to the proposed W-ASG and S-ASG. The RMS values of the tracking errors are given in Table 2.

VI. CONCLUSION

In this paper, we proposed a new WS-ASMC. It designed two new adaptive switching gains, namely, W-ASG and S-ASG. The W-ASG helped to provide a fast convergence rate in the *reaching phase* while guaranteeing the system stability at all times without considering the stability criteria that has always been used in the TDC. The S-ASG helped to improve adjunctively performance in the *reaching phase* while enhancing the system stability near equilibrium point. The nonsingular terminal sliding variable was employed to improve performance in the *sliding phase*. The proposed WS-ASMC used the state information from previous time to cancel the complex nonlinear system model and thus provided a simple structure. From a synergistic effect of these benefits, through the simulation of robot manipulator, the results demonstrated that the proposed WS-ASMC can ensure better tracking performance with enhanced robustness than existing control approaches.

Given that new adaptive switching gains of the proposed WS-ASMC can be easily used in many other applications, we believe that the proposed one will be adopted by a number of researchers. However, when the nonsingular terminal sliding variable (14) used in the proposed WS-ASMC stays far from the equilibrium point, the convergence rate in the *sliding phase* may be slow. As a future work, we will develop a new WS-ASMC based on fast nonsingular terminal sliding variables [34], [35] to address the aforementioned weakness in the proposed WS-ASMC. We think that it would be a good trial to improve the convergence rate further in the *sliding phase*.

APPENDIXES

APPENDIX A

PROOF OF THEOREM 1

In this Appendix, Lyapunov function $V_t \in \Re$ is defined to guarantee the system stability as follows:

$$V_t = \frac{1}{2}\mathbf{s}_t^T\mathbf{s}_t + \frac{1}{2}\sum_{i=1}^{n}\frac{\gamma_i}{\phi_i}\big(\tilde{k}_{i,t}^E\big)^2 + \frac{1}{2}\sum_{i=1}^{n}\frac{1}{\delta_i}\big(\hat{k}_{0,i,t}^S\big)^2 \quad (16)$$

where $\tilde{k}_{i,t}^E = \bar{E}_0^* - \hat{k}_{0,i,t}^E \geq 0$. The time derivative of Lyapunov function can be represented as

$$\begin{aligned}\dot{V}_t &= \mathbf{s}_t^T\dot{\mathbf{s}}_t - \dot{\mathbf{\Lambda}}_{1,t} + \dot{\mathbf{\Lambda}}_{2,t}\\ &= \mathbf{s}_t^T\Big\{\dot{\mathbf{e}}_t + \frac{p}{q}\mathbf{K}_s\big[\mathrm{diag}(\dot{\mathbf{e}}_t^{\frac{p}{q}-1})\big]\ddot{\mathbf{e}}_t\Big\} - \dot{\mathbf{\Lambda}}_{1,t} + \dot{\mathbf{\Lambda}}_{2,t}\\ &= \mathbf{s}_t^T\Big\{\dot{\mathbf{e}}_t + \frac{p}{q}\mathbf{K}_s\big[\mathrm{diag}(\dot{\mathbf{e}}_t^{\frac{p}{q}-1})\big]\big[\ddot{\mathbf{q}}_{d,t} - \ddot{\mathbf{q}}_t\big]\Big\} - \dot{\mathbf{\Lambda}}_{1,t} + \dot{\mathbf{\Lambda}}_{2,t}.\end{aligned} \quad (17)$$

where $\dot{\mathbf{\Lambda}}_{1,t} = \sum_{i=1}^{n}\frac{\gamma_i}{\phi_i}\tilde{k}_{i,t}^E\dot{\hat{k}}_{0,i,t}^E$ and $\dot{\mathbf{\Lambda}}_{2,t} = \sum_{i=1}^{n}\frac{1}{\delta_i}\hat{k}_{0,i,t}^S\dot{\hat{k}}_{0,i,t}^S$. In Eq. (17), the error acceleration is defined as $\ddot{\mathbf{e}}_t = \ddot{\mathbf{q}}_{d,t} - \ddot{\mathbf{q}}_t \in \Re^n$. Substituting Eq. (3) into Eq. (17) yields

$$\begin{aligned}\dot{V}_t = \mathbf{s}_t^T\dot{\mathbf{e}}_t + \mathbf{s}_t^T\Big\{\frac{p}{q}\mathbf{K}_s\big[\mathrm{diag}(\dot{\mathbf{e}}_t)^{\frac{p}{q}-1}\big]\big[\ddot{\mathbf{q}}_{d,t} - \boldsymbol{\vartheta}_t - \bar{\mathbf{M}}^{-1}\boldsymbol{\tau}_t\big]\Big\}\\ -\dot{\mathbf{\Lambda}}_{1,t} + \dot{\mathbf{\Lambda}}_{2,t}.\end{aligned} \quad (18)$$

If Eq. (9) is inserted in Eq. (18), the time derivative of V_t can be obtained as

$$\begin{aligned}\dot{V}_t = \mathbf{s}_t^T\dot{\mathbf{e}}_t + \mathbf{s}_t^T\boldsymbol{\eta}_t\Big\{-\mathbf{E}_t - \frac{q}{p}\mathbf{K}_s^{-1}\dot{\mathbf{e}}_t^{2-\frac{p}{q}}\Big\}\\ -\mathbf{s}_t^T\boldsymbol{\eta}_t\big\{\big[\hat{\mathbf{K}}_t^S + \hat{\mathbf{K}}_t^E\big]\mathrm{sgn}(\mathbf{s}_t)\big\} - \dot{\mathbf{\Lambda}}_{1,t} + \dot{\mathbf{\Lambda}}_{2,t}\end{aligned} \quad (19)$$

where $\boldsymbol{\eta}_t = \frac{p}{q}\mathbf{K}_s\big[\mathrm{diag}(\dot{\mathbf{e}}_t^{\frac{p}{q}-1})\big] = \mathrm{diag}(\eta_{1,t}, \eta_{2,t}, \cdots, \eta_{n,t}) \in \Re^{n\times n}$. $\mathbf{E}_t = \boldsymbol{\vartheta}_t - \hat{\boldsymbol{\vartheta}}_t \in \Re^n$ is defined as the TDE errors. Eq. (19) can be represented as

$$\begin{aligned}&\dot{V}_t\\ &= \sum_{i=1}^{n} s_{i,t}\eta_{i,t}\big\{-E_{i,t} - \hat{k}_{0,i,t}^S s_{i,t}\big\} - \dot{\mathbf{\Lambda}}_{1,t} + \dot{\mathbf{\Lambda}}_{2,t}\\ &\quad - \sum_{i=1}^{n} s_{i,t}\eta_{i,t}\big\{\big[\hat{k}_{0,i,t}^E + \bar{k}_{1,i}\Omega_1 + \bar{k}_{2,i}\Omega_2 + \bar{k}_{3,i}\Omega_3\big]\mathrm{sgn}(s_{i,t})\big\}\end{aligned} \quad (20)$$

where $\Omega_1 = \|\dot{\mathbf{q}}_t\|^2$, $\Omega_2 = \|\ddot{\mathbf{q}}_t - \ddot{\mathbf{q}}_{t-L}\|$, and $\Omega_3 = \|\ddot{\mathbf{q}}_t\|$. From Lemma 2, if time-invariant switching gains in $\hat{k}_{i,t}^E$ (10), *e.g.*, $\bar{k}_{1,i}$, $\bar{k}_{2,i}$, and $\bar{k}_{3,i}$, are chosen to be

$$\bar{k}_{1,i} \geq \bar{E}_1^*,\ \bar{k}_{2,i} \geq \bar{E}_2^*,\ \bar{k}_{3,i} \geq \bar{E}_3^* \quad (21)$$

where $i = 1, 2, \cdots, n$, and then we have

$$\begin{aligned}\dot{V}_t &\leq \sum_{i=1}^{n}|s_{i,t}|\eta_{i,t}\big\{\bar{E}_0^* - \hat{k}_{0,i,t}^E\big\} - \sum_{i=1}^{n}\hat{k}_{0,i,t}^S\eta_{i,t}s_{i,t}^2\\ &\quad - \dot{\mathbf{\Lambda}}_{1,t} + \dot{\mathbf{\Lambda}}_{2,t}\\ &= \sum_{i=1}^{n}|s_{i,t}|\eta_{i,t}\big\{\bar{E}_0^* - \hat{k}_{0,i,t}^E\big\} - \sum_{i=1}^{n}\hat{k}_{0,i,t}^S\eta_{i,t}s_{i,t}^2\\ &\quad - \sum_{i=1}^{n}\tilde{k}_{i,t}^E|s_{i,t}|^{\mathcal{L}_t}\eta_{i,t}\mathcal{L}_t - \sum_{i=1}^{n}\hat{k}_{0,i,t}^S\big(|s_{i,t}|^a + \omega_i|s_{i,t}|^a\mathcal{L}_t\big)\end{aligned} \quad (22)$$

where $\mathcal{L}_t = \mathrm{sgn}(\|\mathbf{s}_t\|_\infty - \varepsilon)$. In Eq. (22), we have two cases: $\|\mathbf{s}_t\|_\infty \geq \varepsilon$ and $\|\mathbf{s}_t\|_\infty < \varepsilon$. If the maximum value

of the sliding variables is larger than the fixed boundedness ε, *i.e.*, $\|\mathbf{s}_t\|_\infty \geq \varepsilon$, it follows then that

$$\begin{aligned}\dot{V}_t &\leq -\sum_{i=1}^{n} \hat{k}^S_{0,i,t}\eta_{i,t}s^2_{i,t} - \sum_{i=1}^{n} \hat{k}^S_{0,i,t}(\omega_i+1)|s_{i,t}|^a \\ &\leq -\sum_{i=1}^{n} \hat{k}^S_{0,i,t}(\omega_i+1)|s_{i,t}|^a. \end{aligned} \tag{23}$$

From (23), it can be represented as follows:

$$\dot{V}_t \leq -\sum_{i=1}^{n} \underline{k}^{*,S}_{0,i}(\omega_i+1)|\varepsilon|^a \leq -\sum_{i=1}^{n} \underline{\rho}_i \tag{24}$$

where $\underline{\rho}_i = \underline{k}^{*,S}_{0,i}(\omega_i+1)|\varepsilon|^a > 0$ is a positive value that exists as the minimum decreasing rate of the Lyapunov function V_t. In other words, the sliding variable $\mathbf{s}_t$ enters a set, *i.e.*, $S = \{\mathbf{s}_t \,|\, \|\mathbf{s}_t\|_\infty < \varepsilon\}$, within a finite time. However, Eq. (22) may not be guaranteed to be negative when $\hat{k}^S_{0,i,t}$ is equal to $\underline{k}^{*,S}_{0,i}$, *i.e.*, $\hat{k}^S_{0,i,t} = \underline{k}^{*,S}_{0,i}$. In this case, Eq. (22) can be described as

$$\begin{aligned}\dot{V}_t &\leq -\sum_{i=1}^{n} \hat{k}^S_{0,i,t}\eta_{i,t}s^2_{i,t} + \sum_{i=1}^{n} \hat{k}^S_{0,i,t}(\omega_i-1)|s_{i,t}|^a \\ &\leq \sum_{i=1}^{n} \hat{k}^S_{0,i,t}(\omega_i-1)|s_{i,t}|^a. \end{aligned} \tag{25}$$

From Eq. (25), let us assume that the Lyapunov function V_t and the magnitude of the sliding variable $s_{i,t}$ are defined as V_1 and $C_{1,i}$ at time $t_1 > 0$, respectively. The maximum increasing rate of the Lyapunov function V_1 is $\sum_{i=1}^{n} \underline{k}^{*,S}_{0,i}(\omega_i - 1)|C_{1,i}|^a$. As the worst case of Eq. (25), it follows that

$$V_2 = V_1 + \sum_{i=1}^{n} \underline{k}^{*,S}_{0,i}(\omega_i-1)|C_{1,i}|^a \tag{26}$$

where V_2 is the Lyapunov function updated by the maximum increasing rate of the Lyapunov function V_1 for time $t_2 > t_1$. As worst case, let us assume that the sliding variable $s_{i,t}$ is defined as $C_{2,i} > C_{1,i}$. The rate of change in the Lyapunov function V_2 is $-\sum_{i=1}^{n}(\underline{k}^n_{0,i} + \bar{\zeta})(\omega_i+1)|C_{2,i}|^a$ where $\bar{\zeta}$ is sufficiently small, and then Eq. (26) can be represented as follows:

$$\begin{aligned}V_3 &= V_2 - \sum_{i=1}^{n}(\underline{k}^{*,S}_{0,i} + \bar{\zeta})(\omega_i+1)|C_{2,i}|^a \\ &< V_1 - \sum_{i=1}^{n} \underline{k}^{*,S}_{0,i}\omega_i\Omega^-_i - \sum_{i=1}^{n} \underline{k}^{*,S}_{0,i}\Omega^+_i \\ &< V_1 - \sum_{i=1}^{n} \underline{k}^{*,S}_{0,i}\Omega^+_i < V_1 - 2\sum_{i=1}^{n} \underline{k}^{*,S}_{0,i}|\varepsilon|^a \end{aligned} \tag{27}$$

where $\Omega^-_i = |C_{2,i}|^a - |C_{1,i}|^a$ and $\Omega^+_i = |C_{2,i}|^a + |C_{1,i}|^a > 2\varepsilon$. The Lyapunov function V_3 is updated by the maximum increasing rate of V_2 for time $t_3 > t_2$. From Eqs. (24) and (27), however, the sliding variable $s_{i,t}$ is steadily decreased toward the sliding manifold. It implies that the sliding variable stays the vicinity of the sliding manifold, *i.e.*, $\|\mathbf{s}_t\|_\infty \geq \varepsilon$, in the finite time $t_\varepsilon \geq t_3$. However, if the sliding variable $\mathbf{s}_t$ stays at a set, *i.e.*, $S = \{\mathbf{s}_t \,|\, \|\mathbf{s}_t\|_\infty < \varepsilon\}$, Eq. (22) may not be guaranteed to be negative. It means that the sliding variable $\mathbf{s}_t$ may escape from the region of $\|\mathbf{s}_t\|_\infty < \varepsilon$. However, the sliding variable $\mathbf{s}_t$ will reach the fixed boundedness ε again owing to Eq. (24).

Now, we will obtain the upper bound of the sliding variable $\mathbf{s}_t$ which can be represented as follows:

$$\frac{1}{2}\|\mathbf{s}_t\|^2 \leq V_t \leq \frac{1}{2}\sum_{i=1}^{n}\varepsilon^2 + \frac{1}{2}\chi_{1,t} + \frac{1}{2}\chi_{2,t} \tag{28}$$

where

$$\begin{aligned}\chi_{1,t} &= \sum_{i=1}^{n} \frac{\gamma_i}{\phi_i}\Big[\max_i\left(\bar{E}^*_{0,i}, |\bar{k}^{*,E}_{0,i} - \bar{E}^*_{0,i}|\right)\Big]^2 \\ \chi_{2,t} &= \sum_{i=1}^{n} \frac{1}{\delta_i}(\bar{k}^{*,S}_{0,i})^2. \end{aligned}$$

From Eq. (28), the sliding variable $\mathbf{s}_t$ is bounded as

$$\|\mathbf{s}_t\| \leq \sqrt{\sum_{i=1}^{n}\varepsilon^2 + \chi_{1,t} + \chi_{2,t}} \tag{29}$$

which implies the uniformly ultimate boundedness. Therefore, the tracking error $\mathbf{e}_t$ in Eq. (14) is also bounded. It follows that the system (Eq. (1)) controlled by the proposed WS-ASMC provides the bounded-input-bounded-output (BIBO) stability [36].

APPENDIX B
PROOF OF LEMMA 1

In this Appendix, we consider the Lyapunov function V_t with a sufficiently large value $\bar{V}^*$ as follows:

$$V_t = \underbrace{\frac{1}{2}\mathbf{s}^T_t\mathbf{s}_t}_{\text{First term}} + \underbrace{\frac{1}{2}\sum_{i=1}^{n}\frac{\gamma_i}{\phi_i}(\tilde{k}^E_{i,t})^2}_{\text{Second term}} + \underbrace{\frac{1}{2}\sum_{i=1}^{n}\frac{1}{\delta_i}(\hat{k}^{*,S}_{0,i,t})^2}_{\text{Third term}} = \bar{V}^*. \tag{30}$$

As the third term of Eq. (30) is bounded by Eq. (13), let's consider the first and second terms of Eq. (30). At least one of them should be sufficiently large, and then the time derivative of Lyapunov function is negative from Eq. (23) if the first term of Eq. (30) is sufficiently large. From another viewpoint, if the second term of Eq. (30) is sufficiently large, we have the optimal problem:

$$\max \sum_{i=1}^{n}\frac{\gamma_i}{\phi_i}\tilde{k}^E_{i,t} \tag{31}$$

subject to

$$\frac{1}{2}\sum_{i=1}^{n}\frac{\gamma_i}{\phi_i}(\tilde{k}^E_{i,t})^2 = N \leq \bar{V}^*$$

where N is a sufficiently large number. The optimal problem in Eq. (31) clearly provides a negative value because N is taken to be sufficiently large. It means that

$$\sum_{i=1}^{n}|s_{i,t}|\eta_{i,t}\{E^*_{0,i} - \hat{k}^E_{0,i,t}\} - \sum_{i=1}^{n}\tilde{k}^E_{i,t}|s_{i,t}|^{\mathcal{L}_t}\eta_{i,t}\mathcal{L}_t < 0 \tag{32}$$

for a sufficiently large N and $\eta_{i,t} \neq 0$ in Eq. (22). In other words, Eq. (22) follows then that

$$\dot{V}_t \leq \sum_{i=1}^{n} |s_{i,t}|\eta_{i,t}\{\bar{E}^*_{0,i} - \hat{k}^E_{0,i,t}\} - \sum_{i=1}^{n} \hat{k}^S_{0,i,t}\eta_{i,t}s^2_{i,t} + \sum_{i=1}^{n} \tilde{k}^E_{i,t}|s_{i,t}|^{-1}\eta_{i,t} + \sum_{i=1}^{n} \hat{k}^S_{0,i,t}(\omega_i - 1)|s_{i,t}|^a < 0. \tag{33}$$

However, when $\eta_{i,t}$ is zero as a special case, *i.e.*, $\eta_{i,t} = 0$, Eq. (33) can be represented as

$$\dot{V}_t \leq \sum_{i=1}^{n} \hat{k}^S_{0,i,t}(\omega_i - 1)|s_{i,t}|^a \leq \sum_{i=1}^{n} \bar{\rho}_i \tag{34}$$

where $\bar{\rho}_i = \bar{k}^{*,S}_{0,i}(\omega_i - 1)\varepsilon^a$ is a positive constant. From Eq. (34), if the first term of Eq. (30) is increased as the worst case, and then $\eta_{i,t}$ has at least any positive value, *i.e.*, $\eta_{i,t} \geq \underline{\eta}_i$ where $\underline{\eta}_i$ is a positive value. It implies that the time derivative of the Lyapunov function in Eq. (33) can be provided as follows:

$$\dot{V}_t < -\sum_{i=1}^{n} \bar{\rho}_i. \tag{35}$$

According to Eqs. (33) and (35), if one of the first and second terms in Eq. (30) is sufficiently large, the time derivative of the Lyapunov function is negative. To be summarized, the Lyapunov function V_t is globally upper-bounded, *i.e.*, $V_t \leq \bar{V}^*$, and hence $\hat{k}^E_{0,i,t}$ has an unknown upper-bound $\bar{k}^{*,E}_{0,i}$ for $t \geq 0$.

APPENDIX C
A TWO-LINK PLANAR ROBOT MANIPULATOR SYSTEM MODEL

We conducted the simulations with a two-link planar robot manipulator [37] whose model is given as

$$\mathbf{M}(\mathbf{q}_t) = \begin{bmatrix} l_2^2 m_2 + 2l_1 l_2 m_2 c_2 + l_1^2(m_1 + m_2) & l_2^2 m_2 + l_1 l_2 m_2 c_2 \\ l_2^2 m_2 + l_1 l_2 m_2 c_2 & l_2^2 m_2 \end{bmatrix}$$

$$\mathbf{C}(\mathbf{q}_t, \dot{\mathbf{q}}_t)\dot{\mathbf{q}}_t = \begin{bmatrix} -m_2 l_1 l_2 s_2 \dot{q}^2_{2,t} - 2m_2 l_1 l_2 s_2 \dot{q}_{1,t}\dot{q}_{2,t} \\ m_2 l_1 l_2 s_2 \dot{q}^2_{2,t} \end{bmatrix}$$

$$\mathbf{G}(\mathbf{q}_t) = \begin{bmatrix} m_2 l_2 g c_{12} + (m_1 + m_2) l_1 g c_1 \\ m_2 l_2 g c_{12} \end{bmatrix}$$

$$\mathbf{F}(\dot{\mathbf{q}}_t) = \begin{bmatrix} \kappa_1 \mathrm{sgn}(\dot{q}_{1,t}) \\ \kappa_2 \mathrm{sgn}(\dot{q}_{2,t}) \end{bmatrix}$$

where $q_{i,t}$ is the angle for the joint i, and s_i, c_i, and c_{ij} are defined by $\sin(q_{i,t})$, $\cos(q_{i,t})$, and $\cos(q_{i,t} + q_{j,t})$, respectively. The system parameters of simulations are introduced in Table 3.

TABLE 3. Parameters of the system for simulation setup.

Axis	Time t (s)	Mass m (kg)	Length l (mm)	Gravity g (m/s^2)	Friction κ
1	$0 \sim 3.77$	10	200	9.81	40
2	$3.77 \sim 13.2$	5	100	9.81	40
	$13.2 \sim 20.0$	3	100	9.81	40

APPENDIX D
PARAMETER TUNING PROCEDURE

Step 1) To begin with, p, q, and $\mathbf{K}_s$ are chosen to provide desirable error dynamics when the TDE errors are assumed to be zero. In general, p and q are set to be 5 and 3, respectively. $\mathbf{K}_s$ is designed to obtain dominant pole, and its initial value is specified as 1.

Step 2) The parameters ϕ_i, γ_i, and ε of the adaptive law (11) are chosen as initial values 1, 1, and 0.1, respectively. Next, the parameters δ_i, ω_i, a, $\underline{k}^{*,S}_{0,i}$, and $\bar{k}^{*,S}_{0,i}$ of the adaptive law (13) are also chosen as initial values 1, 1, 1, 10^3, and 10^4, respectively.

Step 3) After a standard setup, we should check the sliding variable $\mathbf{s}_t$ (14), which can set the boundedness ε less than the maximum value of $\mathbf{s}_t$ while operating the system. Then, ϕ_i and γ_i are tuned to adjust the adaptation rate of the W-ASG. Next, δ_i and ω_i are also tuned to adjust the adaptation rate of the S-ASG. In case of S-ASG, a can be fine-tuned around 1. $\underline{k}^{*,S}_{0,i}$ and $\bar{k}^{*,S}_{0,i}$ are recommended to be determined in consideration of trade-off between chattering and convergence rate.

Step 4) For better convergence rate, all parameters $\bar{k}_{1,i}$, $\bar{k}_{2,i}$, and $\bar{k}_{3,i}$ are tuned by increasing their values from zero. As one of practical methods, $\bar{k}_{1,i}$ is first tuned, and then $\bar{k}_{2,i}$ and $\bar{k}_{3,i}$ are set to be zero. In this way, each parameter can be tuned. Note that they should be set in consideration of trade-off between the sensitivity of states and the convergence rate.

Step 5) To obtain better convergence rate in the *sliding phase*, $\mathbf{K}_s$ is fine-tuned, which offers the better convergence rate in the *sliding phase* as it is larger. However, it should be set in consideration of trade-off between the sensitivity of states and the convergence rate.

Step 6) Please, repeat Step 3) $\sim$ Step 5) once again for achieving the desired level.

REFERENCES

[1] M. Galicki, "Finite-time trajectory tracking control in a task space of robotic manipulators," *Automatica*, vol. 67, pp. 165–170, May 2016.

[2] B. Xiao, S. Yin, and O. Kaynak, "Tracking control of robotic manipulators with uncertain kinematics and dynamics," *IEEE Trans. Ind. Electron.*, vol. 63, no. 10, pp. 6439–6449, Oct. 2016.

[3] D. T. Tran, D. X. Ba, and K. K. Ahn, "Adaptive backstepping sliding mode control for equilibrium position tracking of an electrohydraulic elastic manipulator," *IEEE Trans. Ind. Electron.*, vol. 67, no. 5, pp. 3860–3869, May 2020.

[4] S. Ling, H. Wang, and P. X. Liu, "Adaptive fuzzy tracking control of flexible-joint robots based on command filtering," *IEEE Trans. Ind. Electron.*, vol. 67, no. 5, pp. 4046–4055, May 2020.

[5] C. Ren, X. Li, X. Yang, and S. Ma, "Extended state observer-based sliding mode control of an omnidirectional mobile robot with friction compensation," *IEEE Trans. Ind. Electron.*, vol. 66, no. 12, pp. 9480–9489, Dec. 2019.
[6] K. Youcef-Toumi and O. Ito, "A time delay controller for systems with unknown dynamics," *J. Dyn. Syst., Meas., Control*, vol. 112, no. 1, pp. 133–142, Mar. 1990.
[7] T. C. S. Hsia, T. A. Lasky, and Z. Guo, "Robust independent joint controller design for industrial robot manipulators," *IEEE Trans. Ind. Electron.*, vol. 38, no. 1, pp. 21–25, Feb. 1991.
[8] J. Lee, P. H. Chang, and M. Jin, "Adaptive integral sliding mode control with time-delay estimation for robot manipulators," *IEEE Trans. Ind. Electron.*, vol. 64, no. 8, pp. 6796–6804, Aug. 2017.
[9] J. Kim, H. Joe, S.-C. Yu, J. S. Lee, and M. Kim, "Time-delay controller design for position control of autonomous underwater vehicle under disturbances," *IEEE Trans. Ind. Electron.*, vol. 63, no. 2, pp. 1052–1061, Feb. 2016.
[10] M. Van, H.-J. Kang, and Y.-S. Suh, "Second order sliding mode-based output feedback tracking control for uncertain robot manipulators," *Int. J. Adv. Robotic Syst.*, vol. 10, no. 1, p. 16, Jan. 2013.
[11] Y. Kali, M. Saad, K. Benjelloun, and A. Fatemi, "Discrete-time second order sliding mode with time delay control for uncertain robot manipulators," *Robot. Auto. Syst.*, vol. 94, pp. 53–60, Aug. 2017.
[12] Y. Kali, M. Saad, K. Benjelloun, and C. Khairallah, "Super-twisting algorithm with time delay estimation for uncertain robot manipulators," *Nonlinear Dyn.*, vol. 93, no. 2, pp. 557–569, Mar. 2018.
[13] Y. Kali, J. Rodas, M. Saad, R. Gregor, K. Benjelloun, and J. Doval-Gandoy, "Current control based on super-twisting algorithm with time delay estimation for a five-phase induction motor drive," in *Proc. IEEE Int. Electric Mach. Drives Conf. (IEMDC)*, May 2017, pp. 1–8.
[14] Y. Wang, G. Luo, L. Gu, and X. Li, "Fractional-order nonsingular terminal sliding mode control of hydraulic manipulators using time delay estimation," *J. Vibrat. Control*, vol. 22, no. 19, pp. 3998–4011, Aug. 2016.
[15] Y. Wang, L. Gu, Y. Xu, and X. Cao, "Practical tracking control of robot manipulators with continuous fractional-order nonsingular terminal sliding mode," *IEEE Trans. Ind. Electron.*, vol. 63, no. 10, pp. 6194–6204, Oct. 2016.
[16] J. Baek, M. Jin, and S. Han, "A new adaptive sliding-mode control scheme for application to robot manipulators," *IEEE Trans. Ind. Electron.*, vol. 63, no. 6, pp. 3628–3637, Jun. 2016.
[17] J. Baek, S. Cho, and S. Han, "Practical time-delay control with adaptive gains for trajectory tracking of robot manipulators," *IEEE Trans. Ind. Electron.*, vol. 65, no. 7, pp. 5682–5692, Jul. 2018.
[18] V. Utkin, J. Guldner, and J. Shi, *Sliding Mode Control in Electromechanical Systems*. Boca Raton, FL, USA: CRC Press, 2009.
[19] Y. Feng, X. Yu, and Z. Man, "Non-singular terminal sliding mode control of rigid manipulators," *Automatica*, vol. 38, no. 12, pp. 2159–2167, Dec. 2002.
[20] Y. Wang, L. Liu, D. Wang, F. Ju, and B. Chen, "Time-delay control using a novel nonlinear adaptive law for accurate trajectory tracking of cable-driven robots," *IEEE Trans Ind. Informat.*, to be published, doi: 10.1109/TII.2019.2951741.
[21] Y. Wang, F. Yan, K. Zhu, B. Chen, and H. Wu, "A new practical robust control of cable-driven manipulators using time-delay estimation," *Int. J. Robust Nonlinear Control*, vol. 29, no. 11, pp. 3405–3425, Apr. 2019.
[22] M. Jin, J. Lee, P. Hun Chang, and C. Choi, "Practical nonsingular terminal sliding-mode control of robot manipulators for high-accuracy tracking control," *IEEE Trans. Ind. Electron.*, vol. 56, no. 9, pp. 3593–3601, Sep. 2009.
[23] Y. Wang, K. Zhu, B. Chen, and M. Jin, "Model-free continuous nonsingular fast terminal sliding mode control for cable-driven manipulators," *ISA Trans.*, to be published, doi: 10.1016/j.isatra.2019.08.046.
[24] Y. Wang, F. Yan, J. Chen, F. Ju, and B. Chen, "A new adaptive time-delay control scheme for cable-driven manipulators," *IEEE Trans Ind. Informat.*, vol. 15, no. 6, pp. 3469–3481, Jun. 2019.
[25] T. Hsia, "Simple robust schemes for cartesian space control of robot manipulators," *Int. J. Robot. Autom.*, vol. 9, no. 4, pp. 167–174, 1994.
[26] J. Baek, W. Kwon, B. Kim, and S. Han, "A widely adaptive time-delayed control and its application to robot manipulators," *IEEE Trans. Ind. Electron.*, vol. 66, no. 7, pp. 5332–5342, Jul. 2019.
[27] K. Fu, R. Gonzalez, and G. Lee, *Robotics: Control Sensing Vision*. New York, NY, USA: McGraw-Hill, 1987.
[28] K. Youcef-Toumi and S.-T. Wu, "Input/output linearization using time delay control," *J. Dyn. Syst., Meas., Control*, vol. 114, no. 1, pp. 10–19, Mar. 1992.
[29] S. Jung, T. C. Hsia, and R. G. Bonitz, "Force tracking impedance control of robot manipulators under unknown environment," *IEEE Trans. Control Syst. Technol.*, vol. 12, no. 3, pp. 474–483, May 2004.
[30] C. J. Fallaha, M. Saad, H. Y. Kanaan, and K. Al-Haddad, "Sliding-mode robot control with exponential reaching law," *IEEE Trans. Ind. Electron.*, vol. 58, no. 2, pp. 600–610, Feb. 2011.
[31] O. Barambones and P. Alkorta, "Position control of the induction motor using an adaptive sliding-mode controller and observers," *IEEE Trans. Ind. Electron.*, vol. 61, no. 12, pp. 6556–6565, Dec. 2014.
[32] L. Qiao and W. Zhang, "Double-loop integral terminal sliding mode tracking control for UUVs with adaptive dynamic compensation of uncertainties and disturbances," *IEEE J. Ocean. Eng.*, vol. 44, no. 1, pp. 29–53, Jan. 2019.
[33] B. Armstrong, "Friction: Experimental determination, modeling and compensation," in *Proc. IEEE Int. Conf. Robot. Autom.*, vol.3, Apr. 1988, pp. 1422–1427.
[34] L. Qiao and W. Zhang, "Adaptive second-order fast nonsingular terminal sliding mode tracking control for fully actuated autonomous underwater vehicles," *IEEE J. Ocean. Eng.*, vol. 44, no. 2, pp. 363–385, Apr. 2019.
[35] L. Qiao and W. Zhang, "Trajectory tracking control of AUVs via adaptive fast nonsingular integral terminal sliding mode control," *IEEE Trans Ind. Informat.*, vol. 16, no. 2, pp. 1248–1258, Feb. 2020.
[36] H. Khalil, *Nonlinear Systems*. Upper Saddle River, NJ, USA: Prentice-Hall, 2002.
[37] J. Craig, *Introduction to Robotics: Mechanics and Control*. Upper Saddle River, NJ, USA: Prentice-Hall, 2005.

JAEMIN BAEK (Member, IEEE) received the B.S. degree in mechanical engineering from Korea University, Seoul, South Korea, in 2012, and the Ph.D. degree (M.S.–Ph.D. joint program) in creative IT engineering from the Pohang University of Science and Technology (POSTECH), in 2018.

Since 2018, he has been with the Agency for Defense Development (ADD), Daejeon, South Korea. His main research interests include controller design for nonlinear control, adaptive/robust control, attitude control, gimbal, robotic, and satellite systems.

Dr. Baek is a member of the IEEE Industrial Electronics Society, the IEEE Control Systems Society, and the Institute of Control, Robotics and Systems.

WOOKYONG KWON received the B.S., M.S., and Ph.D. degrees from the Pohang University of Science and Technology (POSTECH), Pohang, South Korea, in 2011, 2012, and 2017, respectively.

He was a Postdoctoral Researcher with the Department of Creative IT Engineering, POSTECH. He is currently a Researcher with the Electronics and Telecommunications Research Institute (ETRI), Daegu, South Korea. His research interests include control and automation, multiobjective control, robot manipulator, and deep learning.

CHANGMOOK KANG (Member, IEEE) received the B.S. and Ph.D. degrees in electrical engineering from Hanyang University, Seoul, South Korea, in 2012 and 2018, respectively.

In 2018, he was with the Agency for Defense Development (ADD), Daejeon, South Korea. He is currently an Assistant Professor with the Department of Electrical Engineering, Incheon National University (INU). His research interests include control theory, autonomous driving, machine learning, and system integration of intelligent vehicles.

Dr. Kang is a member of the IEEE Intelligent Transportation Systems Society, the IEEE Control Systems Society, the Society of Automotive Engineers, the Korean Society of Automotive Engineers, and the Institute of Control, Robotics and Systems.